PAPER

Design and application of piezoelectric biomaterials

IOP Publishing Journal of Physics D: Applied Physics
J. Phys. D: Appl. Phys. **52** (2019) 194002 (10pp) https://doi.org/10.1088/1361-6463/ab0532

Design and application of piezoelectric biomaterials

Hui Yuan[1], Tianmin Lei[1], Yong Qin[1,2], Jr-Hau He[3] and Rusen Yang[1]

[1] School of Advanced Materials and Nanotechnology, Xidian University, Xi'an 710126, People's Republic of China
[2] Institute of Nanoscience and Nanotechnology, School of Physical Science and Technology, Lanzhou University, Lanzhou 730000, People's Republic of China
[3] Division of Computer Electrical and Mathematical Sciences and Engineering, King Abdullah University of Science and Technology, Thuwal 23955-6900, Saudi Arabia

E-mail: rsyang@xidian.edu.cn, qinyong@lzu.edu.cn and jrhau.he@kaust.edu.sa

Received 31 October 2018, revised 29 December 2018
Accepted for publication 7 February 2019
Published 4 March 2019

Abstract

Multifunctional materials have received increasing attention in recent years. Owing to their inherent biological nature and piezoelectric properties, piezoelectric biomaterials are considered as promising candidates for applications in biomedical systems. The rational material design is important to enhance their piezoelectric and biological activity. The recent development of piezoelectric viruses, peptides, and other polymeric biomaterials is reviewed. Fabrication methods, morphological features, and piezoelectric properties of these biomaterials are presented. The effects of growth direction, phase, and polarization of piezoelectric biomaterials on their piezoelectric activity are discussed. The applications of piezoelectric biomaterials in the fields of nanogenerators, energy-storage devices, sensors, and tissue engineering are provided. The challenges and perspective of piezoelectric biomaterials are provided at the end.

Keywords: biomaterial, piezoelectricity, peptide, nanogenerator, sensor, piezotronics, tissue engineering

(Some figures may appear in colour only in the online journal)

1. Introduction

Piezoelectric materials can interconvert mechanical energy and electrical energy. Owing to their good optical, electric, chemical and mechanical properties, piezoelectric materials have been used in nanogenerators [1], supercapacitors [2], sensors [3] and optical devices [4]. Natural materials such as wood, bone, hair, and collagen have been discovered to have piezoelectric properties [5]. However, the weak piezoelectricity limits their applications. Researchers have devoted time to develop ceramics with high piezoelectricity and have found barium titanate ($BaTiO_3$), lead metaniobate and lead zirconate titanate (PZT). Previous reports showed that piezoelectricity of ceramics was affected by intensity of pressure, temperature and humidity, as in Nguyen *et al* [6]. Piezoelectric ceramics often have poor biocompatibility and a brittle nature, which limit their applications in wearable devices and biomedical area.

Biomaterials with biocompatibility, easy preparation, nontoxicity and environmental friendliness have been regarded as promising alternatives. Polarization was first found in asymmetric biological tissue in 1941 [7]. Piezoelectric biomaterials have received increasing attention in recent years. Many researchers have studied their microstructures and phases, and have enhanced their physical and chemical properties by designing molecular structures, fabricating heterostructures and introducing dopants [8]. Reports have showed that the piezoelectric response in biomaterials is directly related to their phase, shape and growth orientation [9, 10]. The piezoelectricity of peptide fibrils and phages in axial direction is stronger than that in the radial direction [10]. Electric charges generated by physical stimulation on piezoelectric biomaterials contribute to bone growth [11], wound healing [12] and tissue regeneration [13]. Thanks to their biocompatibility, nontoxicity, porous structure and good piezoelectricity,

piezoelectric biomaterials have been used for energy storage, energy harvesting and other areas.

In spite of the great advances of piezoelectric biomaterials and their application potential, a comprehensive review of recent development of piezoelectric biomaterial remains lacking. We herein review the growth, characterization and application of piezoelectric biomaterials. We discuss their applications in the fields of nanogenerators, energy-storage devices, sensors and tissue engineering. Moreover, we present their prospect at the end.

2. Material design and characterization

2.1. Piezoelectric virus-based biomaterials

Viruses functionalized through heredity and chemical modification are regarded as promising biofunctional materials. M13 bacteriophage (phage) had a regular rodlike shape, and its length and width were ~880 and of 6.6 nm (figure 1(a)), respectively [14]. The M13 phage was consisted of circular single-stranded DNA packaged with 2700 copies of pVIII major and ~5 copies of pIII, pVI, pVII, and pIX minor coat proteins [15]. Thereinto, the pVIII contained three diverse domains: a hydrophilic N-terminal domain with negative charges, an intermediate hydrophobic domain in middle section, and a positive-charge phage genomic DNA electrostatic interaction domain, respectively [15]. The PVIII proteins with α-helical structure have a dipole moment pointed from the amino-terminal to carboxy-terminal direction and five-fold rotational and double screw symmetry (figures 1(b)–(d)) [16]. M13 phages exhibited a strong piezoelectric response due to their permanent axial polarization caused by the net dipole moment in pVIII proteins [17]. Owing to its hierarchical structure and functional versatility, the M13 phage is widely use in virus-based piezoelectric devices.

M13 phages allow self-assembly into two-dimensional (2D) films and three-dimensional (3D) scaffolds [18]. They enabled biochemical signal display by introducing distinct peptides on component building block through well-established phage-display technology [19, 20]. Highly organized thin films using a nanofibrillar M13 phage as an elementary building block were reported by Rong *et al* [18]. The M13 phage thin films were used to fabricate scaffold to guide cell alignment along a well-defined direction. Engineered M13 phages enabled cell-signaling peptides display on major coat proteins and they were grown into 3D scaffolds to support the differentiation and proliferation of neural progenitor cells [19]. The distinct growth approaches have a significantly influence on the physical and chemical properties of the M13 phase. Self-assembled M13 phage films with liquid-crystalline properties were synthesized by the pulling method or the dropcast method [16]. Piezoelectric strengths of 7.8 pm V^{-1} were measured through piezoresponse force microscopy, and their piezoelectricity was increased by increasing the phage films thickness [16]. Shin *et al* [17] prepared vertically aligned phage nanopillars through infiltrating phage suspension into a porous 3D template with the help of electrostatic interaction. The piezoelectric constant d_{33} for phages nanopillars-type phages was about three times as high as that of film-type phages. The compressive deformation of DNA in the phage nanopillars was believed to contribute to the piezoelectric response in the axial direction of the hyribde materials [17].

2.2. Piezoelectric peptide-based biomaterials

Piezoelectric peptides display the merits of simple preparation, morphological diversity, functional diversity and biocompatibility. Diphenylalanine (FF) is a short dipeptide composed of two phenylalanine through amide-bond formation. The first FF nanotubes were reported in 2003 by Reches and Gazit [21]. They found that the core fragments of β-amyloid protein of FF self-assembled into semi-crystalline nanotubes in an aqueous solution. Those FF nanotubes used amino acids as basic building blocks, showing inherent biocompatibility and special characteristics like high Young modulus [22]. Many researchers have reported various self-assembly processes. Diverse FF structures, including quantum dot, nanosphere, nano/microtube, nanofiber, nanometer/micron capsule, gel and nanoarray, have been developed.

Low-dimension structures of FF-based biomaterials, such as quantum dots and nanocapsules, demonstrated quantum confinement effects on electronic or optical properties. Hybrid colloidal spheres were achieved from cationic FF peptide and polyoxometalte [23]. These spheres were stimuli-responsive to PH and temperature and had adaptive encapsulation properties. Levin *et al* [24] achieved Boc-FF spheres with a metastable phase, and those spheres was transformed into stable crystals. They fabricated different Boc-FF nanostructures by controlling the reaction time and concentration of dipeptide. The Boc-FF spheres were formed after 2 min of reaction in a mixed solution of water and ethanol, owing to Ostwald ripening. When the reaction time increased to 40 and 60 min, the zero-dimension Boc-FF particles were transformed into one-dimension filaments and tubes [24].

FF nanotubes and microrods were widely studied piezoelectric materials that had a non-centrosymmetric space group (P61) [25]. They were self-assembled through vapor deposition or from solution. The vapor deposition approach has been used to grow FF on various substrates. Adler-Abramovich *et al* [26] employed a vapor deposition method to prepare highly aligned aromatic peptide nanotubes (figure 2(a)). Those peptide nanotube arrays were achieved in different lengths, thicknesses and densities. Rosenman *et al* combined physical vapor deposition with photolithography and obtained well-designed patterns of aligned peptide nanotubes array on a wafer (figure 2(b)) [27]. When the FF nanostructures were grown from solution, the solvents and solubility of FF affected their morphologies through the interactions between FF building blocks and the interactions between water and FF building blocks [28]. Kholkin *et al* [29] synthesized in solution FF peptide nanotubes that displayed a piezoelectric constant exceeding 60 pm V^{-1}. In order to achieve large-scale and uniform growth, Nguyen *et al* reported an epitaxial growth approach to fabricate vertically aligned FF microrods on various substrates [30]. The FF microrods (figure 2(c)) exhibited uniform polarization, and the piezoelectric coefficient d_{33}

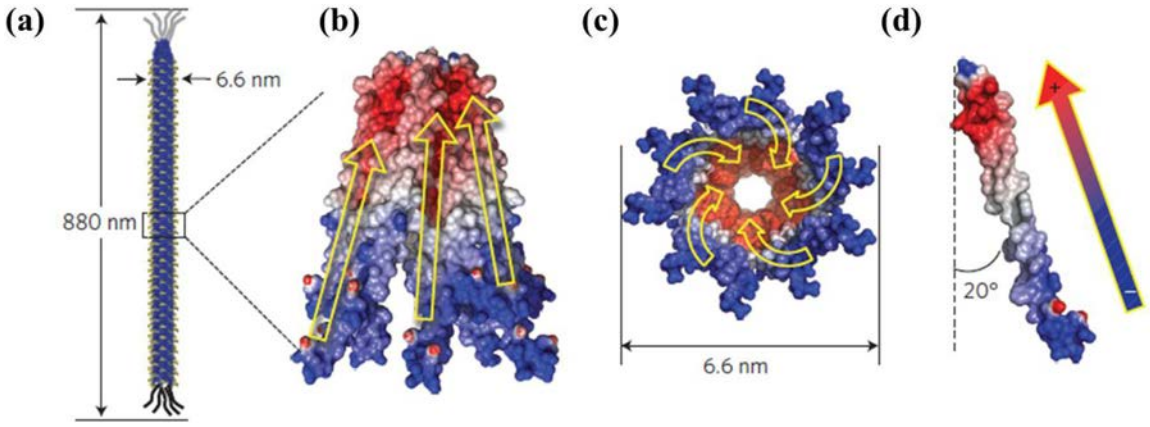

Figure 1. Schematic of M13 phage. (a) A M13 phage with a length of ~880 nm and a diameter of 6.6 nm and covered by ~2700 copies of a major coate protein (pVIII) and fiver copies of minor coat proteins (pIII and pIX). (b) The electrostatic potential of M13 phage. (c) Cross-sectional view of the electrostatic potential of M13 phage. (d) Side-view of the electrostatic potential of a single M13-phage pVIII coat protein. The pVIII coat protein has an ~20° tilt angle with respect to the phage long axis. The colors of the molecular surface indicate positive (red), neutral (white) and negative (blue) electrostatic potentials. Yellow arrows represent the dipole pointing to positive (red) regions from negative (blue). Reprinted with permission from [16].

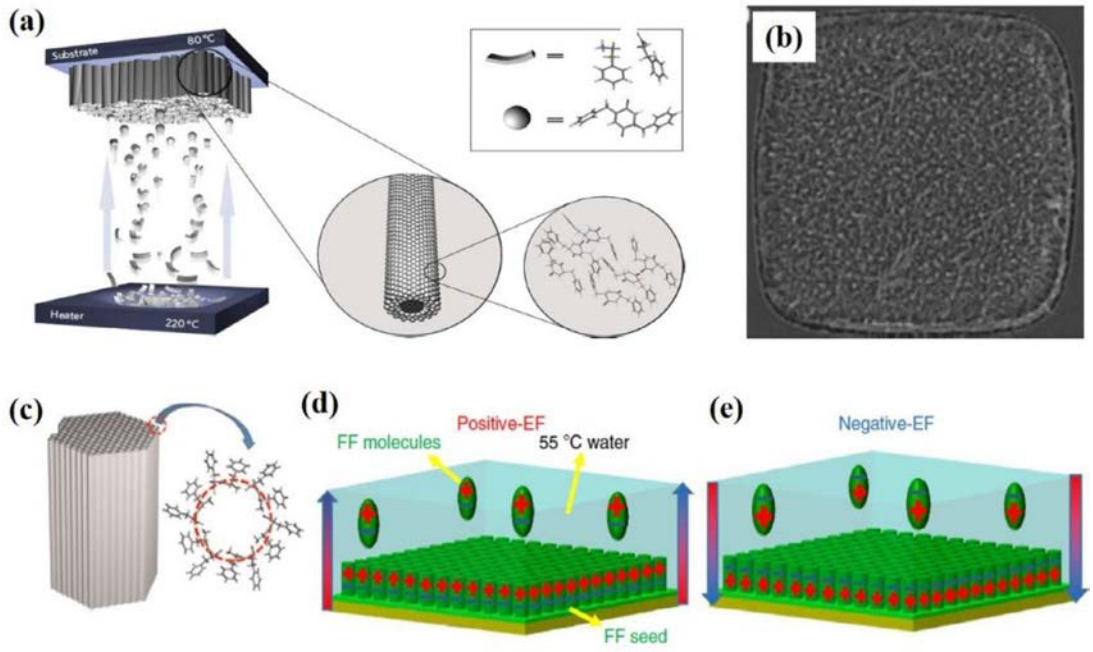

Figure 2. (a) Schematic diagram of the vapor deposition approach.(b) SEM image of peptide nanotubes patterns achieved through physical vapor deposition and photolithography approaches. [27] John Wiley & Sons. Copyright © 2010 European Peptide Society and John Wiley & Sons, Ltd. (c) Schematic diagram for hexagonally arranged nanochannels in an FF microrod. Reprinted from [30], Copyright (2015), with permission from Elsevier. Schematic of growth of FF peptide microrod arrays in (d) positive electric field and (e) negative-electric fields; The large arrows are the directions of the applied electric fields, and the plus and minus signs indicate the polarization of the FF molecules and FF microrod. Reprinted by permission from Macmillian Publishers Ltd: Nature Communications [33], Copyright (2016).

reached 9.9 pm V^{-1}. It was challenging to reverse the polarization of FF nanostructures, which may limit their applications in piezoelectric devices [31]. Molecular dynamics simulation was used to study the aggregation behavior of piezoelectric FF peptides [32]. Research showed that a weak field facilitated the formation of organized FF peptides due to the promotion of the alignment of individual molecular dipole moments. An electric field was confirmed by Nguyen *et al* to control the polarization of FF microrod arrays [33]. When a positive or negative electric field was applied normal to the substrate surface, a controllable and uniform polarization in FF microrods arrays was achieved (figures 2(d) and (e)). The piezoelectric constant in those FF materials exhibited great improvement and reached $d_{33} = 17.9$ pm V^{-1} [33].

Two-dimensional (2D) FF quantum well and three-dimensional (3D) hydrogel have been explored for optical properties. For example, quantum confinement phenomena were observed in FF nanotubes by Amdursky *et al* [4]. 3D scaffolds of peptides hydrogel were formed through gelatinizing to absorb water. Nadav *et al* [34] synthesized FF nanotubes network hydrogel using N-fluorenylmethoxycarbonyl-FF (Fmoc-FF) as building blocks. The Fmoc-FF hydrogel presented optical

absorption and photoluminescence. FF peptides were modified by adding a fluorenyl-methoxycarbonyl (Fmoc) side group, which formed a 3D Fmoc-FF nanofibrils network by molecular stacking [35, 36]. The piezoelectric property in Fmoc-FF fibrous networks was investigated by Ryan *et al* [37] They synthesized Fmoc-FF fibrous networks by a solvent-based method, and the fibrous networks exhibited a shear piezoelectricity due to the noncentrosymmetric β-sheet structure.

2.3. Other piezoelectric biopolymers

Piezoelectric polymers have received significant interest due to their simple structure, flexibility, and promising application in bio-medical area. The mechanism for piezoelectricity in organic materials was reported by Fukada *et al* [38], who proposed that the chiral atomic groups in biomaterial leaded to the piezoelectricity and other optical properties. Polymers such as poly(lacticacid) (PLA), poly-l-lactic acid (PLLA), polyhydroxybutyrate (PHB), polyvinylidene fluoride (PVDF), poly(vinylidene fluoride-trifluoroethylene) (PVDF-TrFE) and polyamide-11 demonstrate piezoelectric properties.

β-phase PVDF films showed one of the highest piezoelectric coefficients among all piezoelectric polymers [39]. Serrado Nunes *et al* [9] prepared α-phase and β-phase PVDF films by a solvent evaporation approach, and studied their piezoelectric activity influenced by phase and morphology. Piezoelectric activity was discovered in β-phase PVDF, and piezoelectric activity was not found in α-phase PVDF. The porous and non-porous structures of the β-phase PVDF films were investigated. The result showed that the piezoelectricity was affected by the porous structure. The piezoelectricity of PVDF films was influenced by its thickness and its dipole moment [40–42]. The 2/3 of the total piezoelectric response in β-phase PVDF was determined by the thickness of the film, and the rest was determined by its different dipolar moments [42].

Great efforts have been devoted to obtain β-phase or increase the content of β-phase in PVDF films. α-phase PVDF films were converted into β-phase by drawing [43]. When applying a draw ratio of 5 at 80 °C, the PVDF films contained the highest percentage of β-phase and exhibited the maximum piezoelectric coefficient values. Compared to PVDF, polyamide 11 has comparable remanent polarizations and coercive fields [44] but lower piezoelectric coefficient [45]. The piezoelectric coefficient in polyamide 11 was less than 4 pC/N at room temperature [46]. But the polyamide 11 presented better thermal stability than PVDF in term of their piezoelectric activity. The piezoelectric activity was still retained up to 170 °C, which was close to its melting range [45].

The macroporous β-PVDF scaffolds were prepared by many strategies such as solvent casting/salt leaching, gel casting, phase separation and emulsion free-drying [47]. Scaffolds with a suitable small porous structure were beneficial for homogeneous cell migration and tissue regeneration [48, 49]. Different morphologies and phases of PVDF were achieved through controlling electrospinning parameters [50]. Various porosities of PVDF-TrFE were obtained by electrospinning [51]. The content of β-phase was controlled by adjusting the applied voltage and rotation speed of the rotation collector [52]. Among them, the rotation speed had more influence on the fraction of β-phase. When the rotation speed increased form 500 rpm to 750 rpm, the β-phase content increased from 45% to 85% [52].

3. Application of piezoelectric biomaterials

3.1. Nanogenerator

Nanogenerators were discovered by Wang *et al* [53] in 2006. They fabricated the first nanogenerator based on aligned ZnO nanowires grown on an α-Al_2O_3 substrate. The discovery of ZnO-based nanogenerators led to many research works in investigating piezoelectric materials for energy harvesting applications. Piezoelectric nanogenerators are based on the piezoelectric effect through which mechanical energy is converted into electricity. Since the discovery of piezoelectric nanogenerators, many other nanogenerators have also been demonstrated, such as triboelectric nanogenerators [54–56] and pyroelectric nanogenerators [57–59]. Piezoelectric biopolymers with a strong piezoelectric response and biological nature were regarded as a promising alternative for the application of a piezoelectric naogenerator. For example, a self-assembled M13 phage was used to fabricate a virus-based piezoelectric naogenerator in 2012, and the nanogenerator produced a current of 6 nA and a voltage of 400 mV [16]. A M13 phage nanopillars-based piezoelectric generator was developed by infiltrating vertically aligned phases into porous templates (figure 3(a)) [17]. The output voltage of M13 phage-based nanogenerators was enhanced by engineering with four negatively charged glutamates (E) phage through a recombinant DNA technology. The 4E phage nanopillar-based piezoelectric nanogenerator generated an average output voltage of 232 mV and a current of 11.1 nA, which were ~3 times higher compared to wild phage nanopillars. M13 phages were used as template to guide the growth of anisotropic $BaTiO_3$ nanocrystals for the fabrication of nanogenerators [60]. This flexible virus-templated $BaTiO_3$ nanogenerator produced a high output voltage of ~6 V and current of ~300 nA (figures 3(b) and (c)) [60].

Peptide-based biomaterials emerged as smart and sustainable materials for electrical energy conversion. For example, Nguyen *et al* [33] reported a power generator based on vertical FF microrod arrays with uniform polarization by applying electric fields (figure 3(d)). The FF-based power generator demonstrated an open-circuit voltage of 1.4 V with an applied force of 60 N (figures 3(e) and (f)), and a power density of 3.3 nW cm^{-2} at 50 MΩ, which was higher than other reported bio-inspired generators and inorganic material-based nanogenerators [61]. An FF-based piezoelectric nanogenerator was integrated with a single-electrode triboelectric nanogenerator to form a hybrid nanogenerator [62]. Polyethylene terephthalate (PET) was chosen as a triboelectric nanogenerator material. The hybrid nanogenerator possessed the advantages of both a piezoelectric nanogenerator and a triboelectric nanogenerator. An enhanced

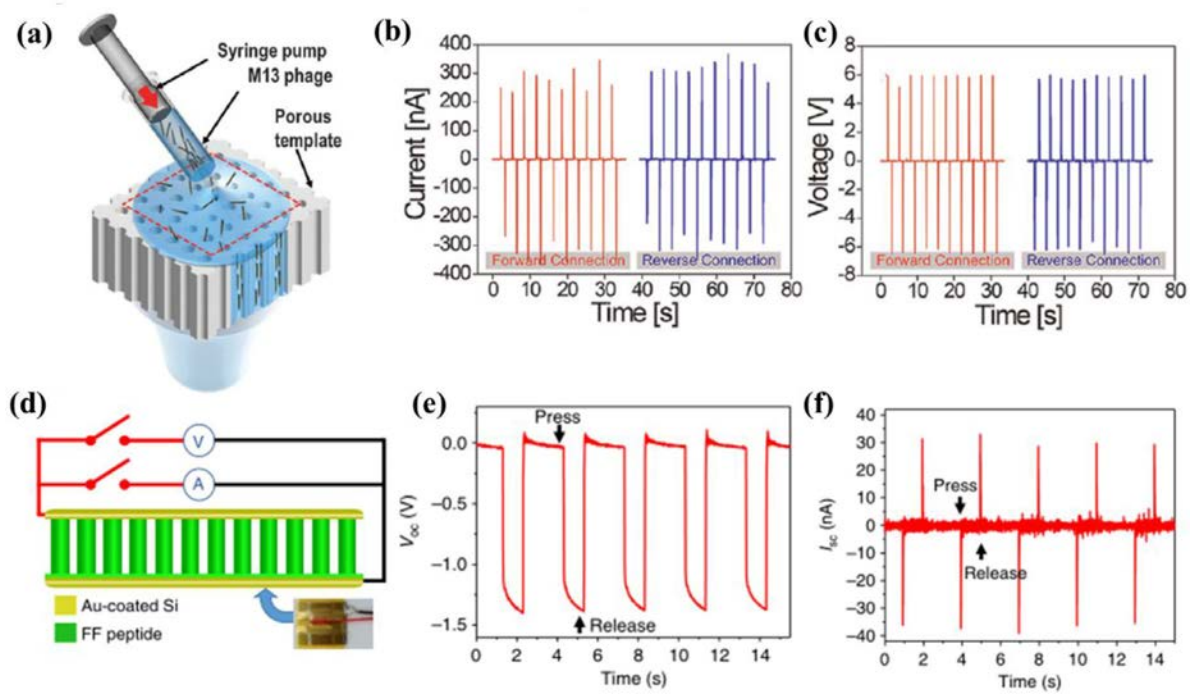

Figure 3. (a) Schematic diagram of assembly for the vertically aligned M13 phage by enforced infiltration. Reprinted from [17] with permission of The Royal Society of Chemistry. Measurement of virus-templated $BaTiO_3$ nanogenerator for (b) short-circuit current and (c) open-circuit voltage in both forward and reverse connections with a 5 cm's curvature radius, 0.3 Hz's frequency, and rate of 0.2 m s^{-1}. Reprinted with permission from [60]. Copyright (2013) American Chemical Society. (d) Schematic of the FF peptide-based nanogenerator connected to the measurement equipment. Bottom-right inset: photography of a real device. (e) Open-circuit voltage and (f) short-circuit current of a FF-based power generator. Reprinted by permission from Macmillan Publishers Ltd: Nature Communciations [33], Copyright (2016).

output voltage of 2.2 V was obtained from the hybrid nanogenerator. A meniscus-driven self-assembly process was reported to synthesize large-scale FF nanotube arrays with an asymmetric shape [63]. The FF nanostructure was adjusted by the type of the solvent, the solubility and pulling speeds. The synthesized FF nanotubes exhibited a high voltage of 2.8 V, a current of 37.4 nA and a power of 8.2 nW, respectively, when a force of 42 N was applied [63].

3.2. Energy storage

Electric double layer capacitor (EDLC) stores energy through reversible adsorption and desorption of charges on electrode surfaces [64]. The specific capacity of EDLC increased with the specific surface area of electrode materials. Piezoelectric biomaterials such as peptides can be used as the electrode for supercapacitors, due to their large specific surface area. Vapor deposition technology has been used to grow FF peptide nanotubes arrays for the electrode of an EDLC [26]. The capacitor based on an aromatic FF nanotubes-modified electrode showed a high areal capacitance of 480 μF cm^{-2} (figure 4(a)), which was four times as high as that of a carbon nanotube-modified electrode and 30 times as high as that of a carbon electrode without any modification. The FF nanotubes-based capacitor demonstrated a high cycle stability and no obvious capacity fade was found after 10 000 charge–discharge cycles [26]. An external electric field was applied to generate unidirectionally aligned and stable FF nanotube/microtube arrays at room temperature [65]. The FF nanotube/microtubes with open ends morphology and multi-layer walls contributed to the large specific surface area. The FF nanostructures were used as electrodes to fabricate a supercapacitor, and a high specific capacity of 1000 μF cm^{-2} at a scan rate of 50 mV s^{-1} was obtained (figure 4(b)).

Piezoelectric biomaterials were used as versatile scaffolds for batteries or catalysts for water oxidation [66, 67]. For examples, Ryu *et al* [68] prepared FF nanowires as scaffolds by treating amorphous thin FF films with aniline vapor at 100 °C for 12 h (figure 4(c)). Co^{2+} absorbed on FF films by preincubating in a $CoCl_2$ aqueous solution. Finally, FF/Co_3O_4 hybrid nanowires were synthesized through reacting Co^{2+} with $NaBH_4$ [68]. These FF/Co_3O_4 hybrid nanowires served as negative electrodes for Li-ion batteries demonstrating good electrochemical performance. Lee *et al* [66] used the major coat protein of E4, a modified M13 virus, as the template for the growth of an amorphous anhydrous iron phosphate (α-$FePO_4$), and the α-$FePO_4$ was grown on multifunctional viruses/single-walled carbon nanotubes (SWNT) as a lithium-ion battery cathode. The lithium-ion batteries showed an excellent performance due to the great affinity of the virus clone toward SWNTs [66].

3.3. Sensor

Piezoelectric biomaterials have been used in biosensors. Various peptide nanostructures were integrated in biosensors

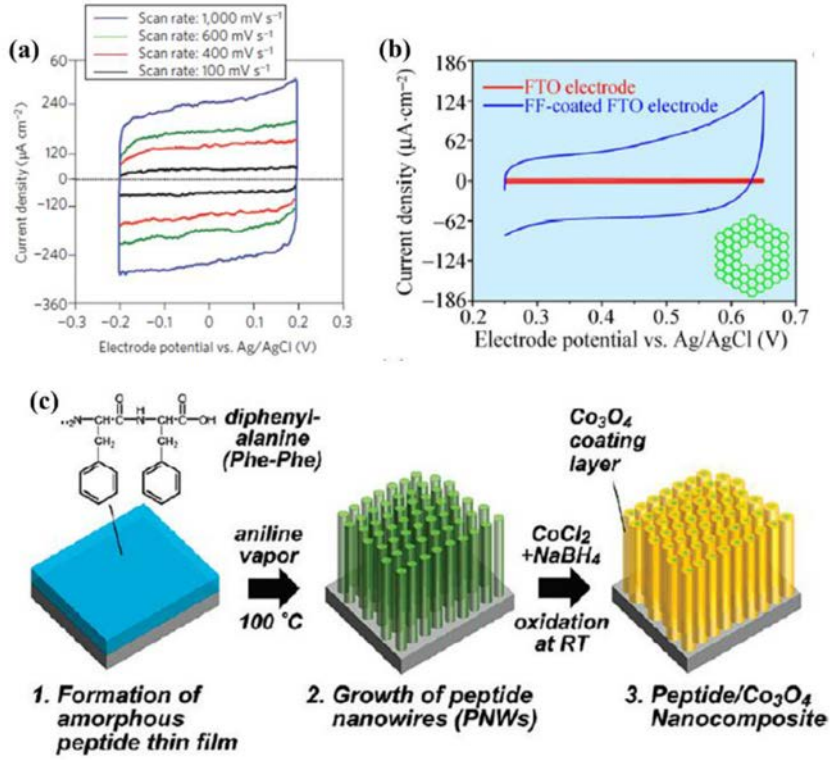

Figure 4. (a) Cyclic voltammogram of an FF nanotubes-modified electrode at different scan rates. Reprinted by permission from Macmillan Publishers Ltd: Nature Communications [26], Copyright (2009). (b) Cyclic voltammogram of a fluorine-doped tin oxide coated glass (FTO) electrode and an FF-coated FTO electrode. The insert demonstrated the porous wall of FF nanotube/microtube. [65] (2014) (© Tsinghua University Press and Springer-Verlag Berlin Heidelberg 2014). With permission of Springer. (c) Schematic diagram of the synthesis of FF/Co_3O_4 hybrid nanowires. Reprinted with permission from [68]. Copyright (2011) American Chemical Society.

to detect phenol, and the sensitivity was significantly improved by the FF pepetide nanoforest that consisted of dense arrays of self-assembled nanostructures [69]. Biosensors with FF nanoforest-coated electrodes were 17 times as sensitive as sensors with uncoated electrodes because of the enormous surface area of the nanoforest. They were also more sensitive than carbon nanotube-modified electrode, FF peptide nanotubes-modified electrode and FF/CNT nanotubes composite-based sensors [69]. FF nanostructure-based sensors were used for cellular detection. Sasso and co-workers reported an amperometric dopamine sensor based on polypyrrole FF nanowire/ polypyrrole [70]. Such sensors reached a high detection limit value of 3.1 μM, which was close to the concentration of dopamine in *in vivo* systems. Additionally, a high value of 100 μA for the amperometric detection of dopamine was obtained.

By virtue of environmental friendliness, simple process and low temperature treatment, 3D printing technology has attracted increasing attention and has widely been applied in fields of energy storages [71], tissue engineering and drug delivery [72]. Recently, 3D printing technology was employed to fabricate a sensor based on 10% of barium titanate ($BaTiO_3$) nanoparticles and β-phase PVDF ball-mill naocomposites. The sensor reported and produced a voltage of 4 V when gentle finger tapped, 10 folds higher than voltage from a film-based sensor [73]. The enhanced performance of the sensor was due to the improvement of inherent piezoelectric properties of the PVDF film. The 10 wt.% $BaTiO_3$ piezoelectric fillers added in PVDF play the role of mechanical activation for the increase of dipole moments [74, 75].

3.4. Tissue engineering

Piezoelectric polymers such as PLA, PHB, PVDF and PVDF-TrFE were often chosen to fabricate scaffolds for cell growth and differentiation in the field of tissue engineering. Among them, PVDF and its co-polymer were the most used biopolymer materials. Nanofibers, films and 3D porous scaffolds have been reported for bone, neural and muscle regeneration [76]. 1D fibers were one of the most frequently adopted materials for tissue engineering (figure 5(a)) [76, 77]. The phase of PVDF fibers synthesized by electrospining was reported to influence the cell growth [78]. Cells exhibited higher alkaline phosphatase activity and earlier mineralization when they grew on PVDF fibers achieved at 25 kV than on PVDF fibers achieved at 12 kV, owing to the higher β-phase fraction (72%) of PVDF fibers achieved at 25 kV [78]. PVDF-TrFE fibrous scaffolds were reported to facilitate the differentiation of mature neural cells [79]. The neurite extension and neuronal differentiation were also stimulated by the piezoelectric effect of PVDF-TrFE scaffolds. During the muscle regeneration, the cell adhesion and proliferation were enhanced by negative charges on the β-PVDF fibrous surface [77]. The elongation of cells along the aligned fibers was induced by oriented fibers, demonstrating their potential for the application in muscle regeneration.

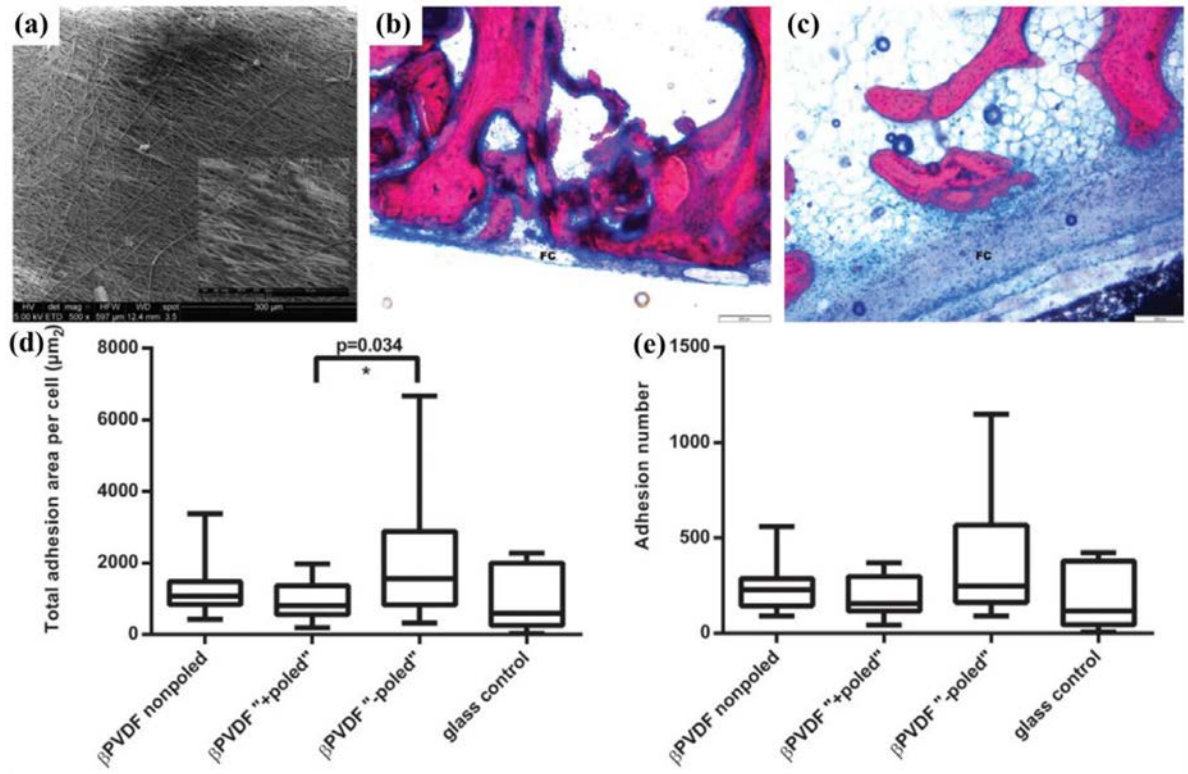

Figure 5. (a) SEM image of aligned electrospun β-PVDF fibers. Reproduced from [77] with permission of The Royal Society of Chemistry. (b), (c) Microphotograph of nondecalcified sections. Reproduced with permission from [81]. On top, (b) exhibits Z3 areas of actuator and (c) exhibits static control, both implanted in the same position in tibia. Total adhesion area (d) and the focal adhesions's number (e) in cells cultured on various substrates after 48 h. [82] John Wiley & Sons. © 2014 Wiley Periodicals, Inc.

Piezoelectric PVDF generated mechanical stimulation when a voltage was applied due to the converse piezoelectric effect. Frias *et al* [80] reported that the mechanical stimulation promoted bone cells growth. When a voltage of 5 V was applied to a piezoelectric PVDF substrate at physiological frequencies of 1 or 3 Hz, new bones were grown *in vivo* on the PVDF substrate. The metabolic activity and gene expression of osteoblasts increased in culture due to the mechanical stimulation [80]. A PVDF-based actuator was implanted in sheep femurs and tibias and produced a mechanical stimulation to the surrounding cells. The rate of new bone growth was higher around the active actuator than a static control sample (figures 5(b) and (c)) [81].

When cells were cultured on PVDF films, the influence of surface charges of the film on the cells adhesion and osteogenic differentiation was observed by Pärssinen *et al* [82]. The cell cultured on 'poled −' β-PVDF increased when compared to cells on the non-poled or 'poled +' PVDF films, because absorbed fibronectin was easily formed on the 'poled −' β-PVDF substrate (figures 5(d) and (e)) [82]. Ribeiro *et al* [83] conducted similar works and used PVDF coated with fibronectin that could promote cell adhesion. The surface charge was produced by mechanical stimuli at 1 Hz. The osteogenic differentiation cultured on 'poled −' β-PVDF films under dynamic conditions was higher than static conditions after 15 d [83]. The result suggested that the electromechanical stimuli could promote the osteogenic differentiation of cells. The piezoelectric PVDF was also used as a substrate for neurons culturing [77, 84]. PVDF substrates with the piezoelectric property produce voltages of 2–3 mV at a frequency of 1200 Hz, and clearly enhanced the outgrowth process of neurons [76].

4. Conclusion and future perspective

Piezoelectric biomaterials are important for both fundamental studies and practical applications. The morphology of peptide materials, the molecular mechanism of physicochemical property, the doping/composite structure, and semiconductor conductivity are of particular research interest. Piezoelectric biomaterials have been applied in the fields of nanogenerators, energy-storage devices, sensors and tissue engineering. In terms of their applications, several aspects are highlighted as follows:

Nanogenerators based on piezoelectric biomaterials such as FF peptides have drawn increasing attention. The nanogenerator with high output and stability is strongly desired. Hence, biomaterials with a strong piezoelectric response and good stability is of great interest for high-performance nanogenerators. Exploring high-piezoelectric response materials by controlling their composition and structure may lead to high-power nanogenerators.

Developing high-performance capacitors based on biomaterials is still a challenge owing to the limitations of their conductivity and chemical activity. Thus, improving the conductivity through surface modification may raise the

performance of biomaterial-based capacitors to a new level. The virus as a template to guide the ordered growth of electrode materials is a promising strategy for a modified supercapacitor or battery.

The application of piezoelectric biomaterials for tissue engineering is an important and under-explored area. These materials can generate electrical or mechanical stimulation through the piezoelectric effect or the converse piezoelectric effect, and both electric and mechanical stimulation were confirmed to enhance the cell growth and differentiation. Piezoelectric biomaterials may serve as a good candidate for the development of biodegradable scaffold for tissue engineering.

Acknowledgments

The authors are genuinely thankful for financial support from Xidian University. Qin thanks the funding support from the National Nature Science Foundation of China (NSFC No. 51472111).

ORCID iDs

Rusen Yang https://orcid.org/0000-0002-4019-4642

References

[1] Gao P X, Song J, Liu J and Wang Z L 2007 Nanowire piezoelectric nanogenerators on plastic substrates as flexible power sources for nanodevices *Adv. Mater.* **19** 67–72
[2] He Y B, Li G R, Wang Z L, Su C Y and Tong Y X 2011 Single-crystal zno nanorod/amorphous and nanoporous metal oxide shell composites: controllable electrochemical synthesis and enhanced supercapacitor performances *Energy Environ. Sci.* **4** 1288–92
[3] Sirohi J 1999 Fundamental understanding of piezoelectric strain sensors *J. Intell. Mater. Syst. Struct.* **11** 246–57
[4] Amdursky N, Molotskii M, Aronov D, Adlerabramovich L, Gazit E and Rosenman G 2009 Blue luminescence based on quantum confinement at peptide nanotubes *Nano Lett.* **9** 3111–5
[5] Fukada E 1983 Piezoelectric properties of biological polymers *Q. Rev. Biophys.* **16** 59–87
[6] Nguyen V, Zhu R and Yang R 2015 Environmental effects on nanogenerators *Nano Energy* **14** 49–61
[7] Martin A J P 1941 Tribo-electricity in wool and hair *Proc. R. Soc.* A **53** 186
[8] Tao K, Makam P, Aizen R and Gazit E 2017 Self-assembling peptide semiconductors *Science* **358** 6365
[9] Nunes J S, Wu A, Gomes J, Sencadas V, Vilarinho P M and Lanceros-Méndez S 2009 Relationship between the microstructure and the microscopic piezoelectric response of the α - and β -phases of poly(vinylidene fluoride) *Appl. Phys.* A **95** 875–80
[10] Minary-Jolandan M and Yu M F 2009 Nanoscale characterization of isolated individual type i collagen fibrils: polarization and piezoelectricity *Nanotechnology* **20** 085706
[11] Frost H M 1994 Wolff's law and bone's structural adaptations to mechanical usage: an overview for clinicians *Angle Orthod.* **64** 175–88
[12] Guo H F, Li Z S, Dong S W, Chen W J, Deng L, Wang Y F and Ying D J 2012 Piezoelectric PU/PVDF electrospun scaffolds for wound healing applications *Colloids Surf.* B **96** 29–36
[13] Zanakis M F and Femano P A 1995 Electrical stimulation technique for tissue regeneration *US Patent Specification* US5433735A
[14] Marvin D A, Welsh L C, Symmons M F, Scott W R P and Straus S K 2006 Molecular structure of fd (f1, M13) filamentous bacteriophage refined with respect to x-ray fibre diffraction and solid-state NMR data supports specific models of phage assembly at the bacterial membrane *J. Mol. Biol.* **355** 294–309
[15] Chung W J, Lee D Y and Yoo S Y 2014 Chemical modulation of M13 bacteriophage and its functional opportunities for nanomedicine *Int. J. Nanomed.* **9** 5825–36
[16] Lee B Y, Zhang J, Zueger C, Chung W J, Yoo S Y, Wang E, Meyer J, Ramesh R and Lee S W 2012 Virus-based piezoelectric energy generation *Nat. Nanotechnol.* **7** 351–6
[17] Shin D M, Han H J, Kim W G, Kim E, Kim C, Hong S W, Kim H K, Oh J W and Hwang Y H 2015 Bioinspired piezoelectric nanogenerators based on vertically aligned phage nanopillars *Energy Environ. Sci.* **8** 3198–203
[18] Rong J, Lee L A, Li K, Harp B, Mello C M, Niu Z and Wang Q 2008 Oriented cell growth on self-assembled bacteriophage M13 thin films *Chem. Commun.* **41** 5185–7
[19] Merzlyak A, Indrakanti S and Lee S W 2009 Genetically engineered nanofiber-like viruses for tissue regenerating materials *Nano Lett.* **9** 846–52
[20] Zhu H, Cao B, Zhen Z, Laxmi A A, Li D, Liu S and Mao C 2011 Controlled growth and differentiation of mscs on grooved films assembled from monodisperse biological nanofibers with genetically tunable surface chemistries *Biomaterials* **32** 4744–52
[21] Reches M and Gazit E 2003 Casting metal nanowires within discrete self-assembled peptide nanotubes *Science* **300** 625–7
[22] Kol N, Adler-Abramovich L, Barlam D, Shneck R Z, Gazit E and Rousso I 2005 Self-assembled peptide nanotubes are uniquely rigid bioinspired supramolecular structures *Nano Lett.* **5** 1343–6
[23] Yan X, Zhu P, Fei J and Li J 2010 Self-assembly of peptide-inorganic hybrid spheres for adaptive encapsulation of guests *Adv. Mater.* **22** 1283–7
[24] Levin A, Mason T O, Adler-Abramovich L, Buell A K, Meisl G, Galvagnion C, Bram Y, Stratford S A, Dobson C M and Knowles T P 2014 Ostwald's rule of stages governs structural transitions and morphology of dipeptide supramolecular polymers *Nat. Commun.* **5** 5219
[25] Ch G 2015 Nanotube formation by hydrophobic dipeptides *Chem. Eur. J.* **7** 5153–9
[26] Adlerabramovich L, Aronov D, Beker P, Yevnin M, Stempler S, Buzhansky L, Rosenman G and Gazit E 2009 Self-assembled arrays of peptide nanotubes by vapour deposition *Nat. Nanotechnol.* **4** 849–54
[27] Rosenman G, Beker P, Koren I, Yevnin M, Bank-Srour B, Mishina E and Semin S 2011 Bioinspired peptide nanotubes: deposition technology, basic physics and nanotechnology applications *J. Pept. Sci.* **17** 75–87
[28] Mason T O, Chirgadze D Y, Levin A, Adlerabramovich L, Gazit E, Knowles T P and Buell A K 2014 Expanding the solvent chemical space for self-assembly of dipeptide nanostructures *ACS Nano* **8** 1243–53
[29] Kholkin A, Amdursky N, Bdikin I, Gazit E and Rosenman G 2010 Strong piezoelectricity in bioinspired peptide nanotubes *ACS Nano* **4** 610–4
[30] Nguyen V, Jenkins K and Yang R 2015 Epitaxial growth of vertically aligned piezoelectric diphenylalanine peptide microrods with uniform polarization *Nano Energy* **17** 323–9

[31] Heredia A, Bdikin I, Kopyl S, Mishina E, Semin S, Sigov A, German K, Bystrov V, Gracio J and Kholkin A L 2010 Fast track communication temperature-driven phase transformation in self-assembled diphenylalanine peptide nanotubes *J. Phys. D: Appl. Phys.* **43** 462001
[32] Kelly C M, Northey T, Ryan K, Brooks B R, Kholkin A, Rodriguez B J and Buchete N V 2015 Conformational dynamics and aggregation behavior of piezoelectric diphenylalanine peptides in an external electric field *Biophys. Chem.* **196** 16–24
[33] Nguyen V, Zhu R, Jenkins K and Yang R 2016 Self-assembly of diphenylalanine peptide with controlled polarization for power generation *Nat. Commun.* **7** 13566
[34] Amdursky N, Gazit E and Rosenman G 2010 Quantum confinement in self-assembled bioinspired peptide hydrogels *Adv. Mater.* **22** 2311–5
[35] Reches M and Gazit E 2005 Self-assembly of peptide nanotubes and amyloid-like structures by charged-termini-capped diphenylalanine peptide analogues *Israel J. Chem.* **45** 363–71
[36] Smith A, Williams R, Tang C, Coppo P, Collins R, Turner M, Saiani A and Ulijn R 2010 Fmoc-diphenylalanine self assembles to a hydrogel via a novel architecture based on π–π interlocked β-sheets *Adv. Mater.* **20** 37–41
[37] Ryan K, Beirne J, Redmond G, Kilpatrick J I, Guyonnet J, Buchete N V, Kholkin A L and Rodriguez B J 2015 Nanoscale piezoelectric properties of self-assembled fmoc–ff peptide fibrous networks *ACS Appl. Mater. Interfaces* **7** 12702–7
[38] Fukada E 1974 Piezoelectric properties of organic polymers *Ann. New York Acad. Sci.* **238** 7–25
[39] Nalwa H S 1995 *Ferroelectric Polymers: Chemistry: Physics, and applications* (CRC Press: New York)
[40] Broadhurst M G, Davis G T, Mckinney J E and Collins R E 1978 Piezoelectricity and pyroelectricity in polyvinylidene fluoride—a model *J. Appl. Phys.* **49** 4992–7
[41] Kepler R G and Anderson R A 1978 Piezoelectricity and pyroelectricity in polyvinylidene fluoride *J. Appl. Phys.* **49** 4490–4
[42] Broadhurst M G and Davis G T 1984 Physical basis for piezoelectricity in PVDF *Ferroelectrics* **60** 3–13
[43] Gomes J, Nunes J S, Sencadas V and Lanceros-Mendez S 2010 Influence of the β-phase content and degree of crystallinity on the piezo- and ferroelectric properties of poly(vinylidene fluoride) *Smart Mater. Struct.* **19** 065010
[44] Kepler R G and Anderson R A 1992 Ferroelectric polymers *Adv. Phys.* **41** 1–57
[45] Takase Y, Lee J W, Scheinbeim J I and Newman B A 1991 High-temperature characteristics of nylon-11 and nylon-7 piezoelectrics *Macromolecules* **24** 6644–52
[46] Frübing P, Kremmer A, Gerhardmulthaupt R, Spanoudaki A and Pissis P 2006 Relaxation processes at the glass transition in polyamide 11: from rigidity to viscoelasticity *J. Chem. Phys.* **125** 214701
[47] Fallahiarezoudar E, Ahmadipourroudposht M, Idris A and Mohd Y N 2015 A review of: application of synthetic scaffold in tissue engineering heart valves *J. Chem. Phys.* **48** 556–65
[48] Nunes-Pereira J, Ribeiro S, Ribeiro C, Gombek C J, Gama F M, Gomes A C, Patterson D A and Lanceros-Méndez S 2015 Poly(vinylidene fluoride) and copolymers as porous membranes for tissue engineering applications *Polym. Test.* **44** 234–41
[49] O'Brien F J, Harley B A, Yannas I V and Gibson L J 2005 The effect of pore size on cell adhesion in collagen-gag scaffolds *Biomaterials* **26** 433–41
[50] Zheng J, He A, Li J and Han C C 2007 Polymorphism control of poly(vinylidene fluoride) through electrospinning *Macromol. Rapid. Commun.* **28** 2159–62
[51] Lee Y-S, Collins G and Livingston Arinzeh T 2011 Neurite extension of primary neurons on electrospun piezoelectric scaffolds *Acta Biomater.* **7** 3877–86
[52] Ribeiro C, Sencadas V, Gómez Ribelles J L and Lanceros-Méndez S 2010 Influence of processing conditions on polymorphism and nanofiber morphology of electroactive poly(vinylidene fluoride) electrospun membranes *Soft Mater.* **8** 274–87
[53] Wang Z L and Song J 2006 Piezoelectric nanogenerators based on zinc oxide nanowire arrays *Science* **312** 242–6
[54] Chen J, Zhu G, Yang W, Jing Q, Bai P, Yang Y, Hou T-C and Wang Z L 2013 Harmonic-resonator-based triboelectric nanogenerator as a sustainable power source and a self-powered active vibration sensor *Adv. Mater.* **25** 6094–9
[55] Niu S, Wang S, Lin L, Liu Y, Zhou Y S, Hu Y and Wang Z L 2013 Theoretical study of contact-mode triboelectric nanogenerators as an effective power source *Energy Environ. Sci.* **6** 3576–83
[56] Cheng L, Xu Q, Zheng Y, Jia X and Qin Y 2018 A self-improving triboelectric nanogenerator with improved charge density and increased charge accumulation speed *Nat. Commun.* **9** 3773
[57] Wang Z L, Zhu G, Yang Y, Wang S and Pan C 2012 Progress in nanogenerators for portable electronics *Mater. Today* **15** 532–43
[58] Lee J-H, Ryu H, Kim T-Y, Kwak S-S, Yoon H-J, Kim T-H, Seung W and Kim S-W 2015 Thermally induced strain-coupled highly stretchable and sensitive pyroelectric nanogenerators *Adv. Energy Mater.* **5** 1500704
[59] Yang Y, Wang S, Zhang Y and Wang Z L 2012 Pyroelectric nanogenerators for driving wireless sensors *Nano Lett.* **12** 6408–13
[60] Jeong C K, Kim I, Park K-I, Oh M H, Paik H, Hwang G-T, No K, Nam Y S and Lee K J 2013 Virus-directed design of a flexible $BaTiO_3$ nanogenerator *ACS Nano* **7** 11016
[61] Xu S, Qin Y, Xu C, Wei Y, Yang R and Wang Z L 2010 Self-powered nanowire devices *Nat. Nanotechnol.* **5** 366
[62] Vu N, Kelly S and Yang R 2017 Piezoelectric peptide-based nanogenerator enhanced by single-electrode triboelectric nanogenerator *APL Mater.* **5** 074108
[63] Ju H L, Heo K, Schulz-Schönhagen K, Ju H L, Desai M S, Jin H E and Lee S W 2018 Diphenylalanine peptide nanotube energy harvesters *ACS Nano* **12** 8138–44
[64] Bonaccorso F, Colombo L, Yu G, Stoller M, Tozzini V, Ferrari A C, Ruoff R S and Pellegrini V 2015 Graphene, related two-dimensional crystals, and hybrid systems for energy conversion and storage *Science* **347** 1246501
[65] Zhang J, Wu X, Gan Z, Zhu X and Jin Y 2014 Unidirectionally aligned diphenylalanine nanotube/microtube arrays with excellent supercapacitive performance *Nano Res.* **7** 929–37
[66] Lee Y J L, Yi H, Kim W-J, Kang K, Yun D S, Strano M S, Ceder G and Belcher A M 2009 Fabricating genetically engineered high-power lithium-ion batteries using multiple virus genes *Science* **324** 1051–5
[67] Nam Y S, Magyar A P, Lee D, Kim J-W, Yun D S, Park H, Pollom T S Jr, Weitz D A and Belcher A M 2010 Biologically templated photocatalytic nanostructures for sustained light-driven water oxidation *Nat. Nanotechnol.* **5** 340
[68] Ryu J, Kim S W, Kang K and Park C B 2011 Synthesis of diphenylalanine/cobalt oxide hybrid nanowires and their application to energy storage *ACS Nano* **4** 159–64
[69] Adler-Abramovich L, Badihi-Mossberg M, Gazit E and Rishpon J 2010 Characterization of peptide-nanostructure-modified electrodes and their application for ultrasensitive environmental monitoring *Small* **6** 825–31

[70] Sasso L, Vedarethinam I, Emnéus J, Svendsen W E and Castillo-León J 2012 Self-assembled diphenylalanine nanowires for cellular studies and sensor applications *J. Nanosci. Nanotechnol.* **12** 3077–83
[71] Karteek K, Mosa I M, Spundana M, Satterwhite-Warden J E, Kuhns T M, Faria R C, Lee N H and Rusling J F 2016 3D-printed supercapacitor-powered electrochemiluminescent protein immunoarray *Biosens. Bioelectron.* **77** 188–93
[72] Xing J F, Zheng M L and Duan X M 2015 Two-photon polymerization microfabrication of hydrogels: an advanced 3D printing technology for tissue engineering and drug delivery *Chem. Soc. Rev.* **44** 5031–9
[73] Bodkhe S, Turcot G, Gosselin F P and Therriault D 2017 One-step solvent evaporation-assisted 3D printing of piezoelectric PVDF nanocomposite structures *ACS Appl. Mater. Interfaces* **9** 20833
[74] Lee D H, Lee J H, Kim D W, Kim B K and Je H J 2010 Enhanced dielectric constant of polymer-matrix composites using nano-$BaTiO_3$ agglomerates *J. Ceram. Soc. Japan* **118** 62–5
[75] Niu Y, Yu K, Bai Y and Wang H 2015 Enhanced dielectric performance of $BaTiO_3$/PVDF composites prepared by modified process for energy storage applications *IEEE Trans. Ultrason. Ferroelectr. Freq. Control* **62** 108–15
[76] Ribeiro C, Sencadas V, Correia D M and Lanceros-Méndez S 2015 Piezoelectric polymers as biomaterials for tissue engineering applications *Colloids Surf.* B **136** 46–55
[77] Martins P M, Ribeiro S, Ribeiro C, Sencadas V, Gomes A C, Gama F M and Lancerosmendez S 2013 Effect of poling state and morphology of piezoelectric poly(vinylidene fluoride) membranes for skeletal muscle tissue engineering *RCS Adv.* **3** 17938–44
[78] Damaraju S M, Wu S, Jaffe M and Arinzeh T L 2013 Structural changes in pvdf fibers due to electrospinning and its effect on biological function *Biomed. Mater.* **8** 045007
[79] Lee Y S and Arinzeh T L 2012 The influence of piezoelectric scaffolds on neural differentiation of human neural stem/progenitor cells *Tissue Eng.* A **18** 2063–72
[80] Frias C, Reis J, Capela e S F, Potes J, Simões J and Marques A T 2010 Polymeric piezoelectric actuator substrate for osteoblast mechanical stimulation *J. Biomech.* **43** 1061–6
[81] Reis J, Frias C, Castro C C E, Botelho M L, Marques A T, Silva F C E and Potes J 2012 A new piezoelectric actuator induces bone formation *in vivo*: a preliminary study *J. Biomed. Biotechnol.* **2012** 613403
[82] Pärssinen J, Hammarén H, Rahikainen R, Sencadas V, Ribeiro C, Vanhatupa S, Miettinen S, Lanceros-Méndez S and Hytönen V P 2015 Enhancement of adhesion and promotion of osteogenic differentiation of human adipose stem cells by poled electroactive poly(vinylidene fluoride) *J. Biomed. Mater. Res.* A **103** 919–28
[83] Ribeiro C, Pärssinen J, Sencadas V, Correia V, Miettinen S, Hytönen V P and Lancerosméndez S 2015 Dynamic piezoelectric stimulation enhances osteogenic differentiation of human adipose stem cells *J. Biomed. Mater. Res. A* **03** 2172–5
[84] Valentini R F, Vargo T G, Gardella J A Jr and Aebischer P 1994 Patterned neuronal attachment and outgrowth on surface modified, electrically charged fluoropolymer substrates *J. Biomater. Sci. Polym. Ed.* **5** 13–36